

Eutectic Salt-Assisted Preparation of Pine Wood-Based N,O Doped Self-Supported Carbon Electrodes for High-Performance Supercapacitors

Songtao Wu^a, Chen Yang^a, Zhenjie Sun^a, Ge Jing^b, Xiaodong You^a, Mingjie Xiong^a, Jialong Chen^a,
Zhenming Li^a, Yuan Liu^a, Hui Li^c, Yunpu Wang^d, Feiqiang Guo^{a,*}

^a School of Low-Carbon Energy and Power Engineering, China University of Mining and Technology,
221116 Xuzhou, China

^b Ningbo CRRC New Energy Technology CO., LTD, Ningbo 315112, China

^c School of Thermal Engineering, Shandong Jianzhu University, Jinan 250101, PR China

^d State Key Laboratory of Food Science and Technology, Engineering Research Center for Biomass
Conversion, Ministry of Education, Nanchang University, Nanchang, 330047, PR China

* Corresponding author. Tel.: +86 516 83592000. E-mail address: fqguo@cumt.edu.cn

1. Characterization

The surface morphology of the samples was characterized using a scanning electron microscope (SEM, Quanta 400 FEG). The submicroscopic structure of the samples was examined by a high-resolution transmission electron microscope (HRTEM, Tecnai G2 F20, FEI, USA). The crystal structure characteristics of the samples were measured with an X-ray diffractometer (XRD, Rigaku Ultima IV, Germany). The defect degree of the samples was studied via a Raman spectrometer (Renishaw RM 2000). A fully automatic specific surface area and pore size analyzer (BET, BD PM-1) was used to determine the specific surface area and pore size distribution of the samples. Moreover, the chemical element composition and valence state information were determined using an X-ray photoelectron spectrometer (XPS, Thermo ESCALAB 250XI, USA).

2. Electrochemical measurements

Cyclic voltammetry (CV), galvanostatic charge-discharge (GCD), and electrochemical impedance spectroscopy (EIS) tests were performed using an electrochemical workstation (CHI, 660E, CN). In the three-electrode system, the prepared KNCW-a was directly used as the working electrode. A standard Hg/HgO electrode served as the reference electrode, and a Pt electrode was used as the counter electrode. A 6 M KOH aqueous solution was employed as the electrolyte. The specific capacitance of the samples can be calculated from the galvanostatic charge-discharge curves using the following formulas (S1-S2):

$$C_s = \frac{I_d \times \Delta t}{\Delta V \times S} \#(S1)$$

$$C_m = \frac{I_d \times \Delta t}{\Delta V \times m} \#(S2)$$

Where C_s (F/cm²) is the areal specific capacitance of the sample, C_m (F/g) is the mass specific capacitance of the sample, I_d (A) is the discharge current, Δt (s) is the discharge time, S is the area of a single electrode, m (g) is the mass of a single electrode, and ΔV (V) is the voltage change during the discharge process.

The energy density E (Wh·kg⁻¹) and power density P (W·kg⁻¹) of the device under two-electrode configuration were calculated as follows:

$$E = \frac{C \times \Delta V^2}{7.2} \text{ (S3)}$$

$$P = \frac{E \times 3600}{\Delta t} \text{ (S4)}$$

where C (F·cm⁻²) is the specific capacitance of the device, ΔV (V) is the discharge voltage of the device, and Δt (s) is the discharge time of the device.

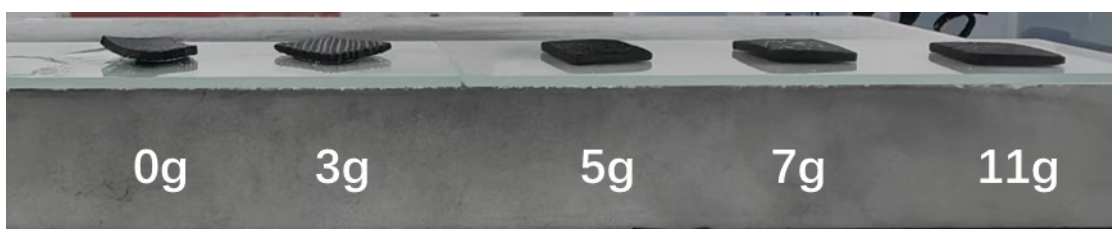


Fig. S1 Variation of the mass of the products under different impregnation concentrations

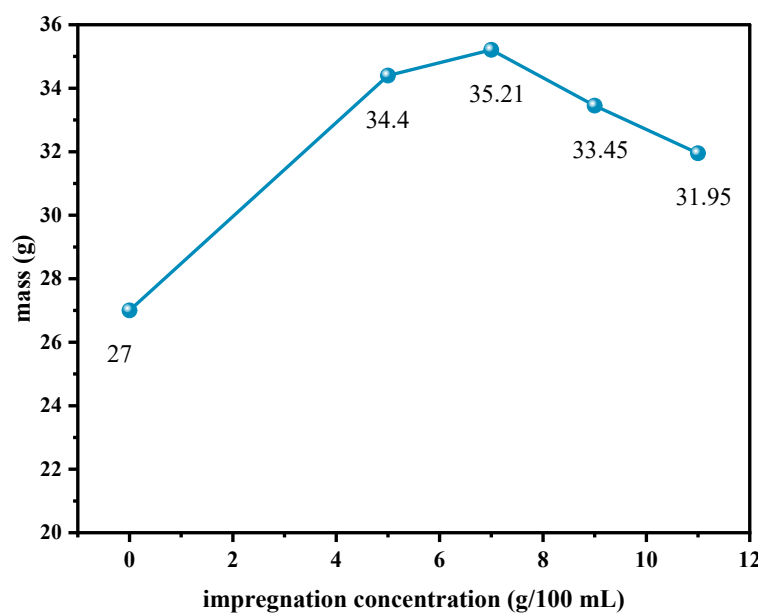


Fig. S2 Variation of the mass of the products under different impregnation concentrations

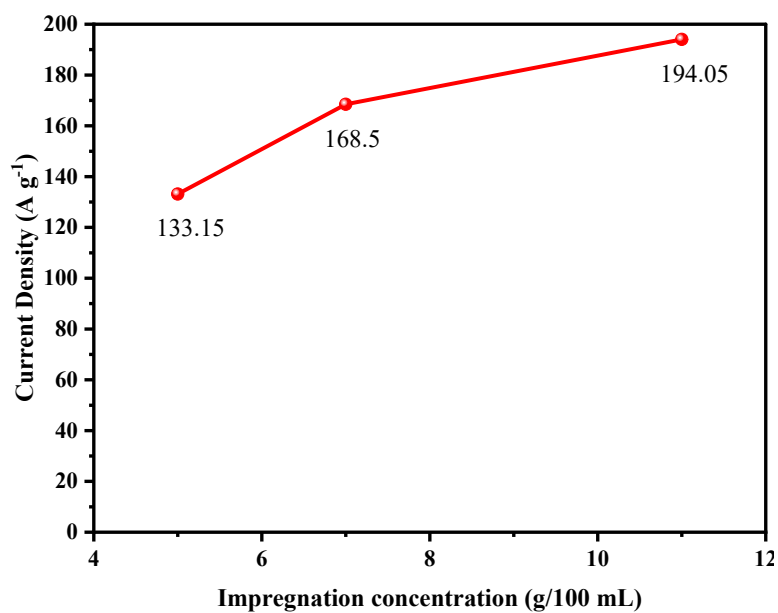


Fig. S3 Variation of the mass specific capacitance of the products under different impregnation concentrations

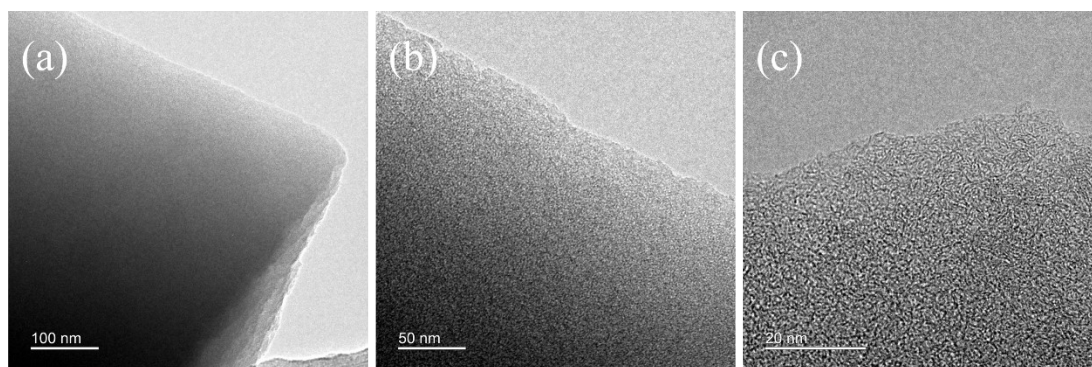


Fig. S4 (a-c) HRTEM images of KNCW-7

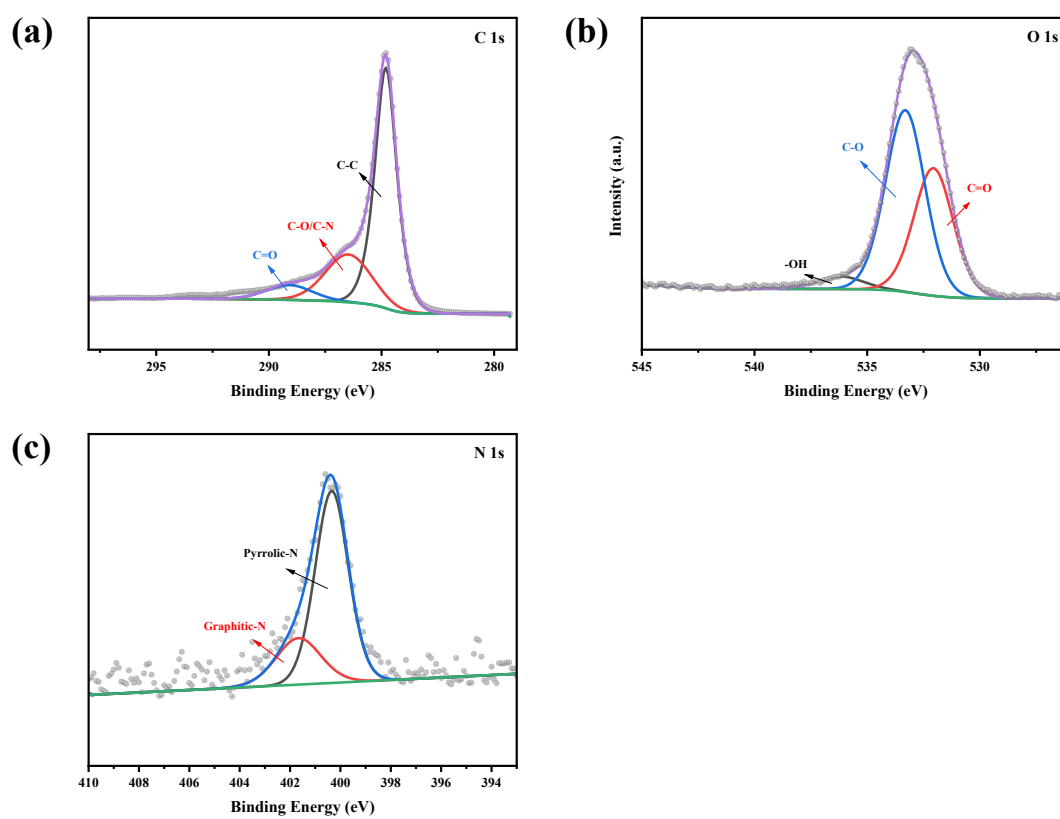


Figure S5 (a) C 1s, (b) O 1s, (c) N 1s XPS spectra of KNCW-0.

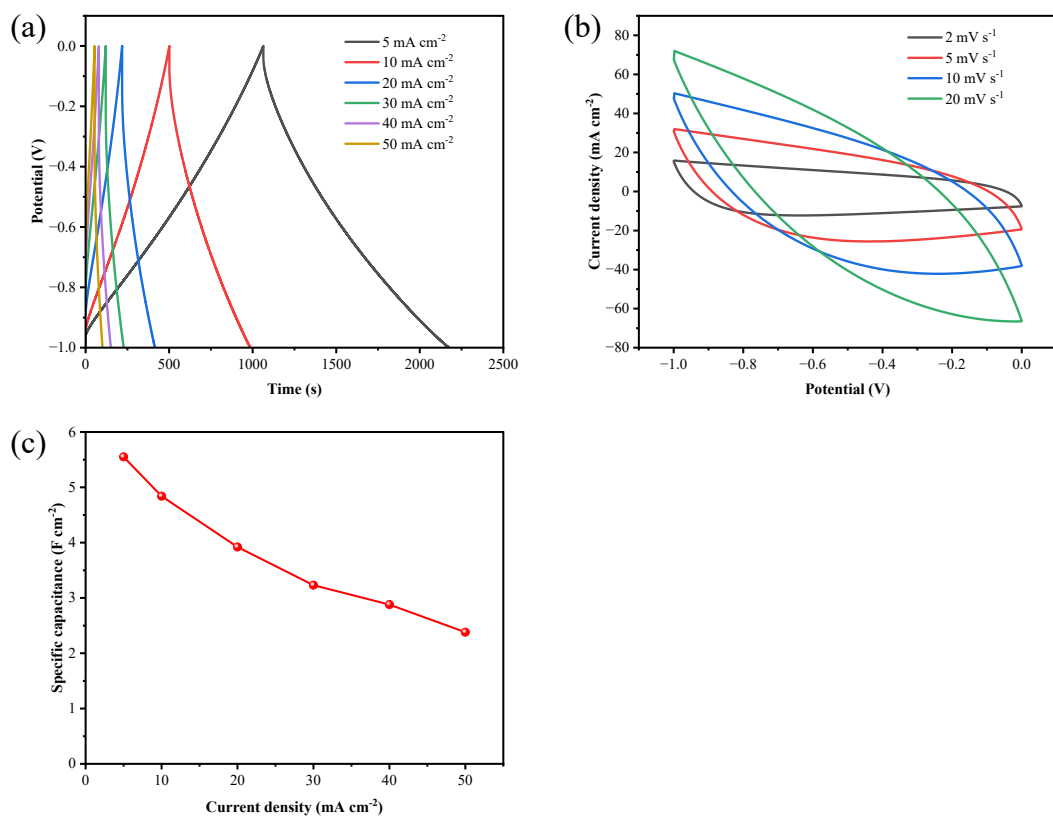


Fig. S6 (a) GCD curves of KNCW-7 at different current densities; (b) CV curves of KNCW-7 at different scan rates; (c) specific capacitances at 5-50 mA·cm⁻²

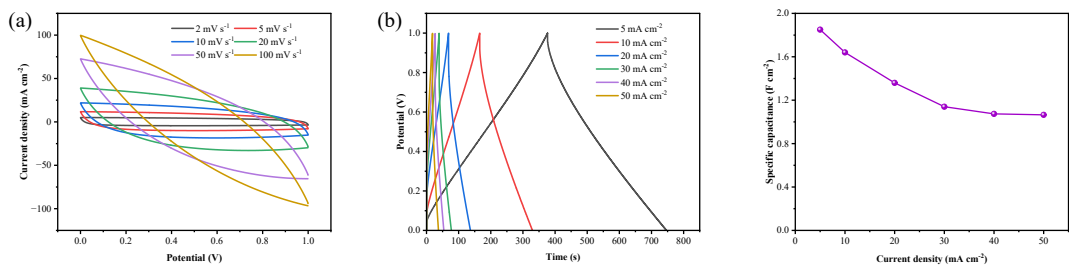


Fig. S7 Electrochemical performances of the KNCW-7//KNCW-7 device in Na₂SO₄: (a) CV curves at various scan rates, (b) GCD curves at different current densities, (c) specific capacitances at 5-50 mA·cm⁻²

Table S1. Comparison of KNCW-7 with previous wood-based carbon electrodes.

Samples and wood species	Areal Capacitance (F cm ⁻²)	Electrolyte	Ref.
CW-Fe-5 (Pine wood)	3.64 F cm ⁻² (5 mA cm ⁻²)	6 M KOH	1
WC@H@K-850-20 (paulownia wood)	7.12 F cm ⁻² (1 mA cm ⁻²)	6 M KOH	2
PWCK2(Ochroma lagopus wood)	6.64 F cm ⁻² (5 mA cm ⁻²)	3 M KOH	3
K20Na15 (Basswood)	3.246 F cm ⁻² (1 mA cm ⁻²)	6 M KOH	4
FA-OC (Basswood)	4.346 F cm ⁻² (2 mA cm ⁻²)	6 M KOH	5

HRGO@CW-1 (poplar)	4.68 F cm ⁻² (5 mA cm ⁻²)	6 M KOH	6
PMCS (Basswood)	2.622 F cm ⁻² (3 mA cm ⁻²)	1 M H ₂ SO ₄	7
KNCW-7 (Pine wood)	7.42 F cm ⁻² (5 mA cm ⁻²)	6 M KOH	This work
	5.55 F cm ⁻² (5 mA cm ⁻²)	1 M Na ₂ SO ₄	

Table S2. E-factor of KNCW-a.

Samples and wood species	E-factor
KNCW-0	3.62
KNCW-5	2.96
KNCW-7	2.99
KNCW-11	3.69

References

1. K. Dong, Z. Sun, J. Wang, G. Jing, L. Kong, B. Tang, S. Wu, X. Huang, X. You, Y. Liu and F. Guo, *Journal of Power Sources*, 2024, **623**.
2. W. Wang, Y. Shen, Z. Ma, X. Wei, H. Fan and Q. Bai, *Sustainable Materials and Technologies*, 2024, **40**.
3. Z. Guo, Z. Tian, Y. Liu, Y. Huang, W. Li, X. Han, S. He, H. Mao, C. Zhang, G. Duan and S. Jiang, *Chem Commun (Camb)*, 2025, **61**, 6474-6477.
4. M. Wang, L. He, Y. Chen and J. Gao, *Journal of Energy Storage*, 2025, **130**.
5. B. Yan, J. Zheng, L. Feng, C. Du, S. Jian, W. Yang, Y. A. Wu, S. Jiang, S. He and W. Chen, *Biochar*, 2022, **4**.
6. L. Fan, J. Sun, H. Shi, H. Qu, J. Yang, C. Li, J. Mu, X. Zhou and L. Sheng, *Journal of Energy Storage*, 2025, **117**.
7. M. Chen, S. Zhu, S. Wang, W. Yang, M. Ye, Y. Zhou, S. Jiang, S. He and J. Han, *Journal of Alloys and Compounds*, 2025, **1037**.